Journal of Orthopaedic Translation 33 (2022) 153–161

Contents lists available at ScienceDirect

Journal of Orthopaedic Translation

journal homepage: www.journals.elsevier.com/journal-of-orthopaedic-translation

Biodegradable magnesium implant enhances angiogenesis and alleviates medication-related osteonecrosis of the jaw in rats

Wang-yong Zhu [a], Jiaxin Guo [b], Wei-fa Yang [a], Zhuo-ying Tao [a], Xinmiao Lan [a], Leilei Wang [a], Jiankun Xu [b], Ling Qin [b], Yu-xiong Su [a,*]

[a] Division of Oral and Maxillofacial Surgery, Faculty of Dentistry, The University of Hong Kong, Hong Kong Special Administrative Region
[b] Musculoskeletal Research Laboratory of Department of Orthopaedics & Traumatology and Innovative Orthopaedic Biomaterial and Drug Translational Research Laboratory, Li Ka Shing Institute of Health, The Chinese University of Hong Kong, Hong Kong Special Administrative Region, China

ARTICLE INFO

Keywords:
Angiogenesis
Biodegradable implants
Bisphosphonate
Magnesium
Medication-related osteonecrosis of the jaw

ABSTRACT

Background: Medication-related osteonecrosis of the jaw (MRONJ) is a serious complication associated with antiresorptive and antiangiogenic medications, of which impaired angiogenesis is a key pathological alteration. Since Magnesium (Mg)-based implants possess proangiogenic effects, we hypothesized that the biodegradable Mg implant could alleviate the development of MRONJ via enhancing angiogenesis.

Methods: MRONJ model was established and divided into the Veh + Ti group (Vehicle-treated rat, with Titanium (Ti) implant), BP + Ti group (Bisphosphonate (BP)-treated rat, with Ti implant), BP + Mg group (BP-treated rat, with Mg implant), BP + Mg + SU5416 group (BP-treated rat, with Mg implant and vascular endothelial growth factor (VEGF) receptor-2 inhibitor), BP + Mg + BIBN group (BP-treated rat, with Mg implant and calcitonin gene-related peptide (CGRP) receptor antagonist), and BP + Mg + SU5416+BIBN group (BP-treated rat, with Mg implant and VEGF receptor-2 inhibitor and CGRP receptor antagonist). The occurrence of MRONJ, alveolar bone necrosis, new bone formation and vessel formation were assessed by histomorphometry, immunohistochemistry, and micro-CT analysis.

Results: Eight weeks after surgery, the BP + Mg group had significantly reduced occurrence of MRONJ-like lesion and histological osteonecrosis, increased bone microstructural parameters, and increased expressions of VEGFA and CGRP, than the BP + Ti group. By simultaneously blocking VEGF receptor-2 and CGRP receptor, the vessel volume and new bone formation in the BP + Mg group were significantly decreased, meanwhile the occurrence of MRONJ-like lesion and histological bone necrosis were significantly increased.

Conclusion: Biodegradable Mg implant could alleviate the development of MRONJ-like lesion, possibly via upregulating VEGF- and CGRP-mediated angiogenesis. Mg-based implants have the translational potential to be developed as a novel internal fixation device for patients with the risk of MRONJ.

The Translational potential of this article: This work reports a biodegradable Mg implant which ameliorates the development of MRONJ-like lesions possibly due to its angiogenic property. Mg-based implants have the potential to be developed as a novel internal fixation device for patients at the risk of MRONJ.

1. Introduction

Antiresorptive and antiangiogenic medications, such as bisphosphonates (BPs) and receptor activator of nuclear factor-κB ligand inhibitors, are mostly used for treating osteopenia and osteoporosis as well as for preventing and treating skeletal-related events associated with bone metastases in patients with cancer [1,2]. Medication-related osteonecrosis of the jaw (MRONJ) is a serious complication associated with use of antiresorptive and antiangiogenic medications, with an incidence ranging from 0.3% to 5% [3–7]. The treatment of MRONJ is challenging. Although more pieces of evidence have emerged to support the use of surgery to treat MRONJ [1,2,8], the success rate of surgical treatment for MRONJ ranges from 58.5% to 75.2% [9–11], and the risk of recurrent or secondary MRONJ is still significant [12–14]. Therefore, new methods of management for MRONJ are desirable.

To date, the advantages of magnesium (Mg) implants to bone fixation

* Corresponding author.
E-mail address: richsu@hku.hk (Y.-x. Su).

https://doi.org/10.1016/j.jot.2022.03.004
Received 3 December 2021; Received in revised form 26 February 2022; Accepted 12 March 2022

and regeneration have been fully validated in various clinical indication-orientated animal models, and the biodegradability and pro-osteogenic function make Mg implant a promising internal fixation device for orthopaedic surgery [15–17]. Our previous work demonstrated that Mg ions derived from the implants enhance the synthesis of calcitonin gene-related peptide (CGRP) at dorsal root ganglia and its release in the periosteum, and CGRP-mediated pathway is the major mechanism underlying Mg-promoted bone regeneration [18]. CGRP is a strong proangiogenic growth factor contributing to bone development and remodeling [19], and our recent study showed that Mg implants applied in distraction osteogenesis present the angiogenic effect via CGRP-focal adhesion kinase (FAK)- vascular endothelial growth factor (VEGF) signaling axis [20].

Since inhibition of angiogenesis caused by antiresorptive and antiangiogenic medications is one of the potential mechanisms underlying MRONJ pathophysiology [1,21], the proangiogenic effect of Mg implant might antagonize the adverse effect of antiresorptive and antiangiogenic medications locally, and the biodegradability of Mg is another ideal property to avoid the surgical trauma of device removal which may trigger secondary MRONJ. Therefore, we hypothesized that the biodegradable Mg implant could alleviate the development of MRONJ via enhancing angiogenesis. In this study, we established an animal model simulating a MRONJ-risk factor in patients who are going to undergo jaw surgery. We aimed to investigate the effects of Mg on the occurrence and histological osteonecrosis of MRONJ-like lesion, and the role of VEGF- and CGRP-mediated angiogenesis under the pathogenesis of MRONJ, thus providing a piece of evidence for the design of Mg-based devices in the surgical management of challenging MRONJ.

2. Materials and methods

2.1. Establishment of animal models

MRONJ model was established in 50 male Sprague Dawley rats (8-week-old), with an average weight of 376 g (ranging from 309 to 450 g). Rats were divided into 6 groups (shown in Table 1): (1) Veh + Ti group (Vehicle-treated rat, implanted with a titanium (Ti) rod in the mandible; 5 rats in total), (2) BP + Ti group (BP-treated rat, implanted with a Ti rod in the mandible; 15 rats in total), (3) BP + Mg group (a pure Mg rod, fabricated following the published protocol [18], was implanted into the mandible of BP-treated rat; 15 rats in total), (4) BP + Mg + SU5416 group (BP-treated rat, implanted with a Mg rod in the mandible and injected with VEGF receptor-2 inhibitor SU5416 (100 μM, 0.1 ml/48 h) for 8 week s; 5 rats in total), (5) BP + Mg + BIBN group (BP-treated rat, implanted with a Mg rod in the mandible and injected with CGRP receptor antagonist BIBN4096BS (300 μg/kg, every 48 h) for 2 weeks; 5 rats in total), (6) BP + Mg + SU5416+BIBN group (BP-treated rat, implanted with a Mg rod in the mandible, then injected with VEGF receptor-2 inhibitor SU5416 (100 μM, 0.1 ml/48 h) and CGRP receptor antagonist BIBN4096BS (300 μg/kg, every 48 h) for 8 and 2 weeks, respectively; 5 rats in total).

Table 1
Study design.

Group	Animals (n/group)	Treatment	Euthanasia
Veh + Ti	5	Saline for 5 weeks Surgery with Ti implant	8 weeks after surgery
BP + Ti	10 + 5	ZA + DX for 5 weeks Surgery with Ti implant	8 weeks after surgery
BP + Mg	10 + 5	ZA + DX for 5 weeks Surgery with Mg implant	8 weeks after surgery
BP + Mg + SU5416	5	ZA + DX for 5 weeks Surgery with Mg implant VEGF receptor-2 inhibitor for 8 weeks	8 weeks after surgery
BP + Mg + BIBN	5	ZA + DX for 5 weeks Surgery with Mg implant CGRP receptor antagonist for 2 weeks	8 weeks after surgery
BP + Mg + SU5416+BIBN	5	ZA + DX for 5 weeks Surgery with Mg implant VEGF receptor-2 inhibitor for 8 weeks, and CGRP receptor antagonist for 2 weeks	8 weeks after surgery

Ti, titanium; ZA, zoledronic acid; DX, dexamethasone; Mg, magnesium; VEGF, vascular endothelial growth factor; CGRP, calcitonin gene-related peptide.

Each rat received once-weekly intraperitoneal injections of zoledronic acid (ZA; 130 μg/kg) and dexamethasone (DX; 3.8 mg/kg), or vehicle (saline), for 5 weeks. These doses were converted from human doses of ZA (4 mg/person/3 weeks) and DX (40 mg/person/week) according to the National Institute of Health guidelines [22]. One week after completion of ZA and DX combination therapy, all rats were subjected to surgical interventions. Rats were anesthetized by intraperitoneal injection with ketamine (60 mg/kg) and xylazine (10 mg/kg). With an extra-oral incision parallel to the inferior border of the left mandible, subcutaneous tissues and masseter muscle were elevated to expose the mandible. A penetrating mandibular tunnel with a diameter of 1.3 mm was made around the first molar root apex with a fissure bur at low speed and copious saline irrigation, then a 1 mm wide bone defect was made below the drilling hole. A sterilized Ti or Mg rod (diameter = 1.3 mm, length = 3 mm) was inserted into the penetrating canal. After the extra-oral incision was closed, the left mandibular 1st molar was removed by dental forceps and the alveolar socket was cleaned using a round bur to remove any remaining root fragments (Fig. 1A). The rats were housed in an environmentally controlled animal-care laboratory after surgery, given analgesia with subcutaneous injection of buprenorphine (0.03 mg/kg) for three consecutive days. Eight weeks after surgery, animals were sacrificed using intraperitoneal injection of pentobarbital (200 mg/kg), and then samples were collected and fixed with 10% buffered formalin. Microcomputed tomography (micro-CT) analysis for new bone formation in bone defect, micro-CT based angiography for new vessel formation, H&E staining for alveolar bone necrosis, immunohistochemistry (IHC) staining for evaluating expressions of VEGFA and CGRP, were conducted.

All animal procedures described above were performed with a protocol approved by the University Ethics Committee on the Use of Live Animals in Teaching and Research (CULATR No. 4835–18) of the University of Hong Kong.

2.2. Criteria for MRONJ-like lesion

The determination of MRONJ-like lesion in each animal was diagnosed by the following histological criteria [1,23]: (1) presence of ulcerative lesion with exposed and necrotic bone and/or osteolysis, and (2) presence of sequestrum. The occurrence rates of MRONJ-like lesions were compared among groups.

2.3. Micro-CT based bone analysis

At week 4 and week 8 after surgery, each animal was scanned using a micro-CT (Skyscan1076, Aartselaar, Belgium) under anesthesia. The acquisition settings were at a pixel size of 17.3 μm with an X-ray tube voltage of 88 kVp and an intensity current of 100 μA. Microarchitectural properties of the newly-formed bone in the mandibular bone defect were evaluated within a conforming volume of interest (VOI), defined as a 3 × 3 × 1 mm^3 volume in the bone defect. Tissue volume (TV; mm^3), bone volume (BV; mm^3), percentage of bone volume (BV/TV; %), bone mineral density (BMD; g HA/cm^3), trabecular thickness (Tb.Th; mm), trabecular number (Tb.N; #/mm), and trabecular separation (Tb.Sp; mm), were calculated.

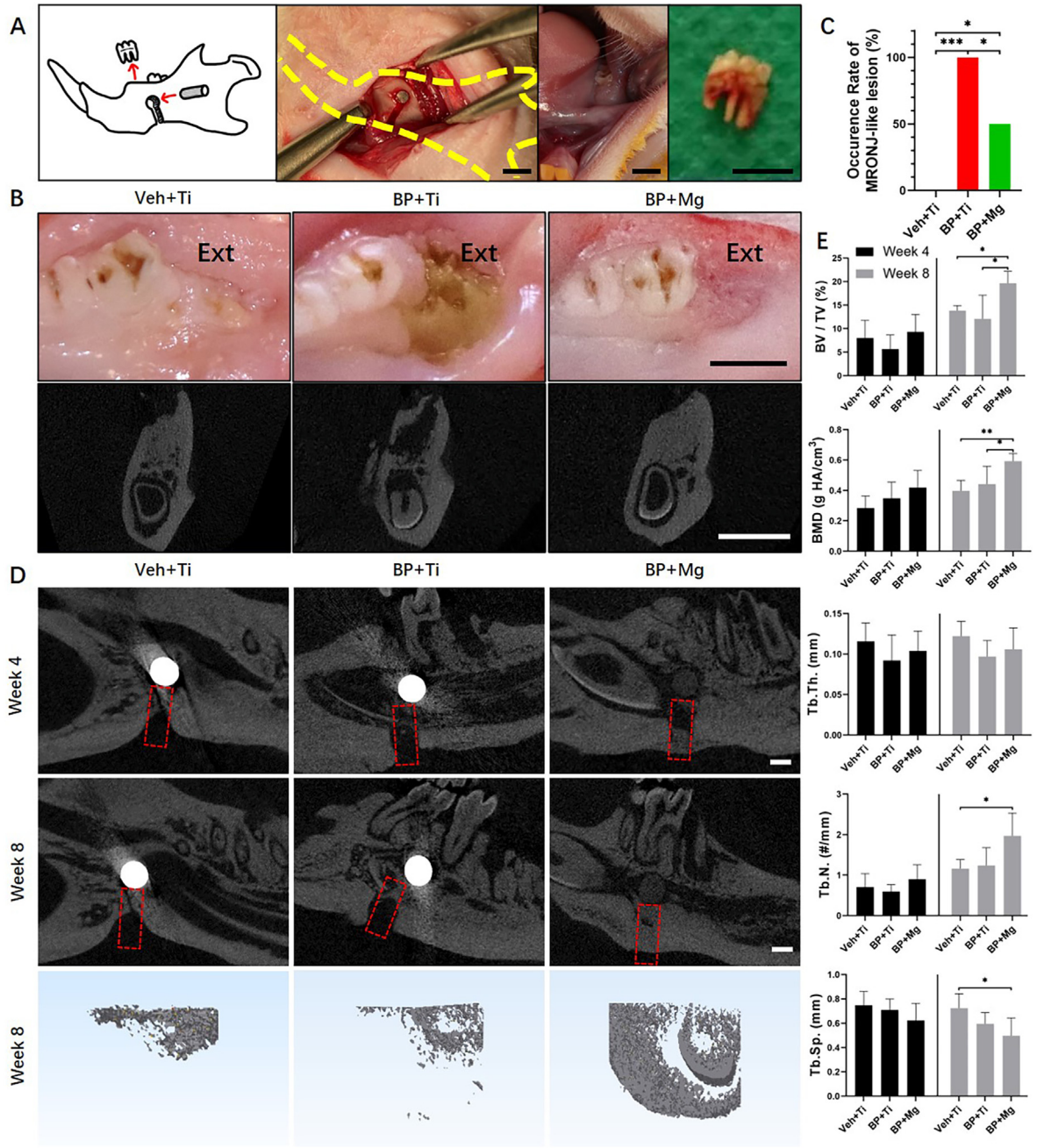

Fig. 1. BP + Mg group presented alleviated MRONJ occurrence and enhanced bone defect repair as compared to the BP + Ti group (A) Schematic and intraoperative images of surgical procedures for establishing the MRONJ model with implant fixation, bone defect creation and dental extraction. A Mg rod (with a purity of 99.99%, 3 mm in length, and 1.3 mm in diameter) or a Ti rod (pure titanium, the same size with Mg rod) was implanted into the mandible; a 1 mm-wide bone defect was cut inferior to the implantation site; the mandibular 1st molar was extracted. Scale bar: 3 mm (B) Representative photos and coronal micro-CT images of extraction sites (Ext) at 8 weeks after surgery, showing complete healing mucosae (Left and Right) and a MRONJ-like lesion with exposure of necrotic bone and sequestrum (Middle). Scale bar: 3 mm (C) Occurrence rate of MRONJ-like lesion in three groups at 8 weeks after surgery. Veh + Ti group n = 5, BP + Ti group n = 9, and BP + Mg group n = 10, by Chi-square test (D) Representative sagittal micro-CT images and 3D reconstructed coronal images of mandibular bone defect (red dotted box) in three groups, 4 weeks and 8 weeks postoperatively. Scale bar: 1 mm (E) Bone micro-architectural morphometric assessment on the newly formed bone in the defect at 4 weeks and 8 weeks after surgery by micro-CT. Column and bar indicate mean and SD, respectively. n = 5 for each group, by One-way ANOVA with Bonferroni *post hoc* test. *, $p < 0.05$. **, $p < 0.01$. ***, $p < 0.001$.

2.4. Micro-CT based angiography

Microfil perfusion was performed in the mandible of the rats in each group (n = 5). Under anesthesia, prewarmed 10 ml heparin (50 IU/ml), 60 ml saline, and 10 ml 10% formalin were sequentially injected into the left cervical artery to clear and fix vessels in mandible, followed by the injection of 10 ml liquid compound (Microfil MV-122; Flow-Tech, Carver, MA, USA). Then the rats were euthanized with overdose of anesthetics. The cadavers were store at 4 °C overnight. The harvested mandibles were decalcified with 15% EDTA for 4 weeks and then scanned using a micro-CT (Skyscan1172, Aartselaar, Belgium). The acquisition settings were at a pixel size of 14.9 μm with an X-ray tube voltage of 80 kVp and an intensity current of 100 μA. An entire region of the mandible (756 slices; each slice = 14.9 μm) was scanned for each animal.

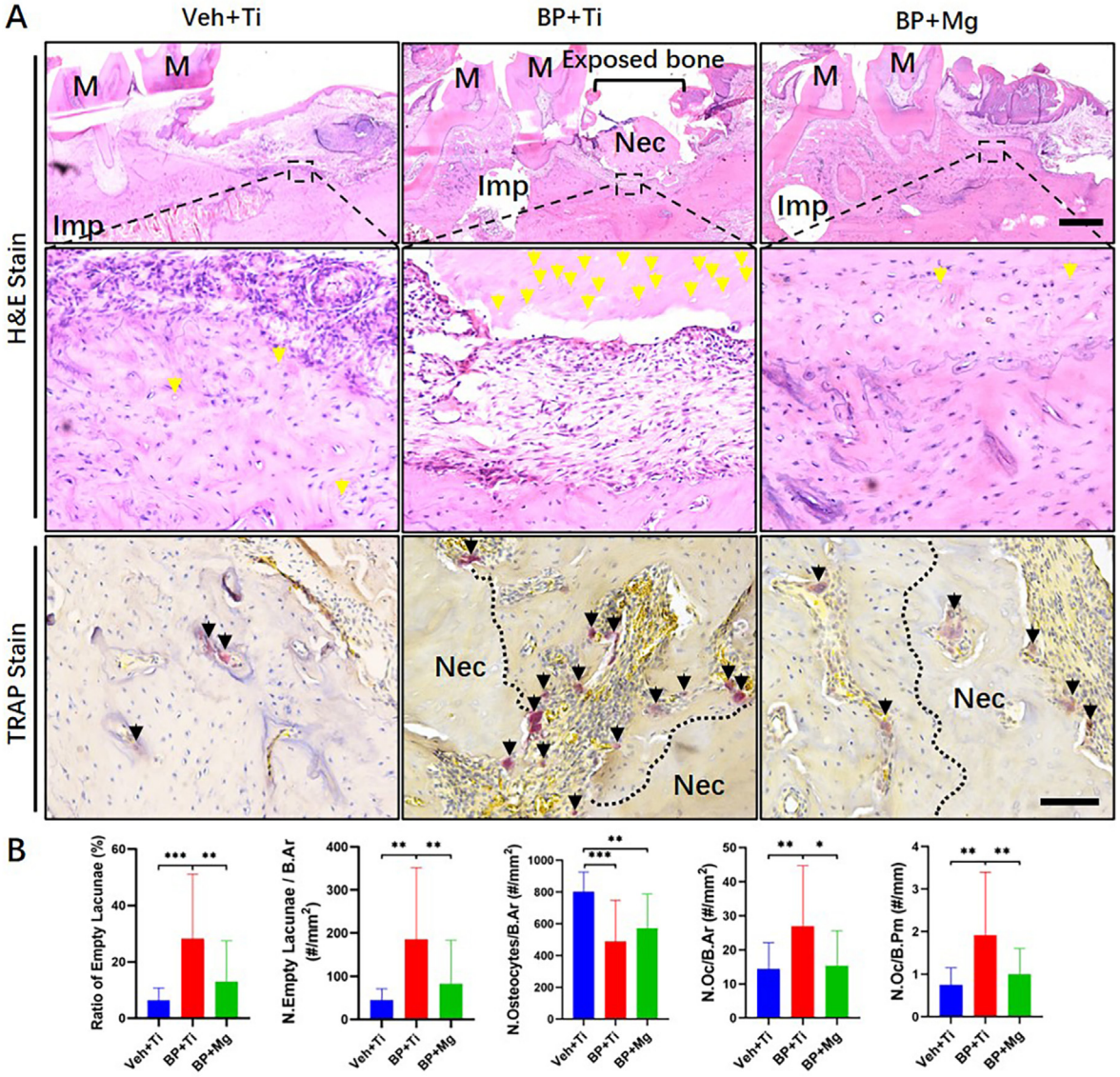

Fig. 2. Comparison of histological osteonecrosis and TRAP-positive osteoclasts at MRONJ-like lesions (A) Representative H&E staining and TRAP staining images of extracted tooth socket 8 weeks after removal in three groups. Imp, implant. M, molar. Nec, necrotic bone. Yellow arrow points the empty lacunae. Black arrow points the TRAP-positive stained osteoclast. Scale bar in H&E stain: 1 mm. Scale bar in TRAP stain: 100 μm (B) Histomorphometric assessments of H&E staining on the degree of alveolar bone necrosis, and TRAP staining on the number of TRAP-positive cells among groups. Column and bar indicate mean and SD, respectively. Veh + Ti group n = 5, BP + Ti group n = 9, and BP + Mg group n = 10, by One-way ANOVA with Bonferroni *post hoc* test. *, $p < 0.05$. **, $p < 0.01$. ***, $p < 0.001$.

The vessels with the infused radiopaque substance were defined at a grey threshold ranging from 50 to 255. Quantitative analysis was performed to evaluate the volume of the vessels per tissue volume (Vessel V/TV; %), vessels thickness (Vessel.Th; mm), and vessels number (Vessels.N; #/mm), within the mandible region.

2.5. Histological and histomorphometric analysis

Harvested samples were decalcified in 15% EDTA for 4–6 weeks at room temperature and then dehydrated in a series of ethanol and xylene before embedding in paraffin. Sections with a thickness of 6 μm were prepared for H&E staining, tartrate-resistant acid phosphatase (TRAP) staining (#387 A-1 KT, Sigma–Aldrich), and IHC staining. In each section focusing on the site of extraction, 3 randomly chosen fields (200 × magnification) were examined, excluding sequestrated and separated bone fragments. To quantify the degree of alveolar bone necrosis, the ratio of empty lacunae to total osteocyte lacunae, the number of empty lacunae per bone area (N.Empty Lacunae/B.Ar), the number of osteocytes per bone area (N.Osteocytes/B.Ar), the number of osteoclasts per bone area (N.Oc/B.Ar), and the number of osteoclasts per bone surface perimeter (N.Oc/B.Pm), were calculated and compared among groups. Expressions of VEGFA, CGRP and CD31 were evaluated by anti-VEGFA primary antibody (ab231260, Abcam), anti-CGRP primary antibody (ab47027, Abcam) and anti-CD31 primary antibody (AF3628, R&D).

2.6. Statistical analysis

All statistics were calculated using SPSS Statistics (version 26.0; IBM Corporation, Chicago, IL, USA) and GraphPad Prism (version 8.0; GraphPad Software Inc, San Diego, CA, USA). Data were presented as mean with standard deviation (SD). Chi-square test was used for comparing the difference of occurrence rate of MRONJ-like lesions among groups. One-way ANOVA with Bonferroni's *post hoc* tests were used in the comparisons of micro-CT bone analysis, angiography, and

histomorphometric analysis. P < 0.05 was considered statistically significant.

3. Results

3.1. Mg alleviated MRONJ-like lesion development and enhanced bone defect repair

In this part, 14 rats survived without adverse events, except one in BP + Ti group died after surgery. Eight weeks after surgery, incidences of MRONJ-like lesion diagnosed by histological criteria in Veh + Ti, BP + Ti and BP + Mg groups were 0%, 100% and 50%, respectively. Dental extraction sites of the BP + Ti group had significantly higher occurrence of MRONJ-like lesions than the Veh + Ti group and BP + Mg group (Fig. 1B and C). Micro-CT bone analysis showed enhanced bone defect repair in the BP + Mg group than the Veh + Ti and BP + Ti groups (Fig. 1D and E). At week 8, newly formed bone in the defect of the BP + Mg group had significantly increased BV/TV and BMD than the BP + Ti group, and significantly increased BV/TV, BMD, Tb.N. and reduced Tb. Sp. than the Veh + Ti group. No significant difference in bone defect repair was observed between the Veh + Ti and BP + Ti groups.

The alleviation of MRONJ-like lesions by Mg was also indicated by the histology results (Fig. 2). Evaluation of H&E and TRAP stained sections of the extraction site was carried out at 8 weeks after surgery. The BP + Ti group had a significantly higher ratio of empty lacunae, N. Empty Lacunae/B.Ar, N. Oc/B.Ar, and N. Oc/B.Pm, than the Veh + Ti and BP + Mg groups. The Veh + Ti and BP + Mg groups had no significant difference in alveolar bone necrosis.

3.2. VEGFA and CGRP might play important roles in Mg-alleviated MRONJ-like lesion development

Eight weeks after surgery, in the BP + Mg group, the alveolar bone region presented significantly higher expressions of VEGFA (p < 0.001) and CGRP (p < 0.001) than the Veh + Ti group and BP + Ti group, indicated by IHC results (Fig. 3). Negative controls of IHC without primary antibodies were shown in supplemental data (Appendix Fig. 1A). In the vessel-like tissue indicated by highly expressed CD31 staining, positive areas of VEGFA and CGRP were frequently observed near the Mg implant.

3.3. By simultaneously blocking VEGF receptor-2 and CGRP receptor, Mg lost the effects of angiogenesis and coupled osteogenesis in MRONJ

In this part, 33 of 35 rats survived without adverse events, 2 rats in BP + Ti and BP + Mg groups died after surgery. The representative 3D reconstructed images demonstrated that more vessels and mineralized bone were found in the BP + Mg group, BP + Mg + SU5416 group, and

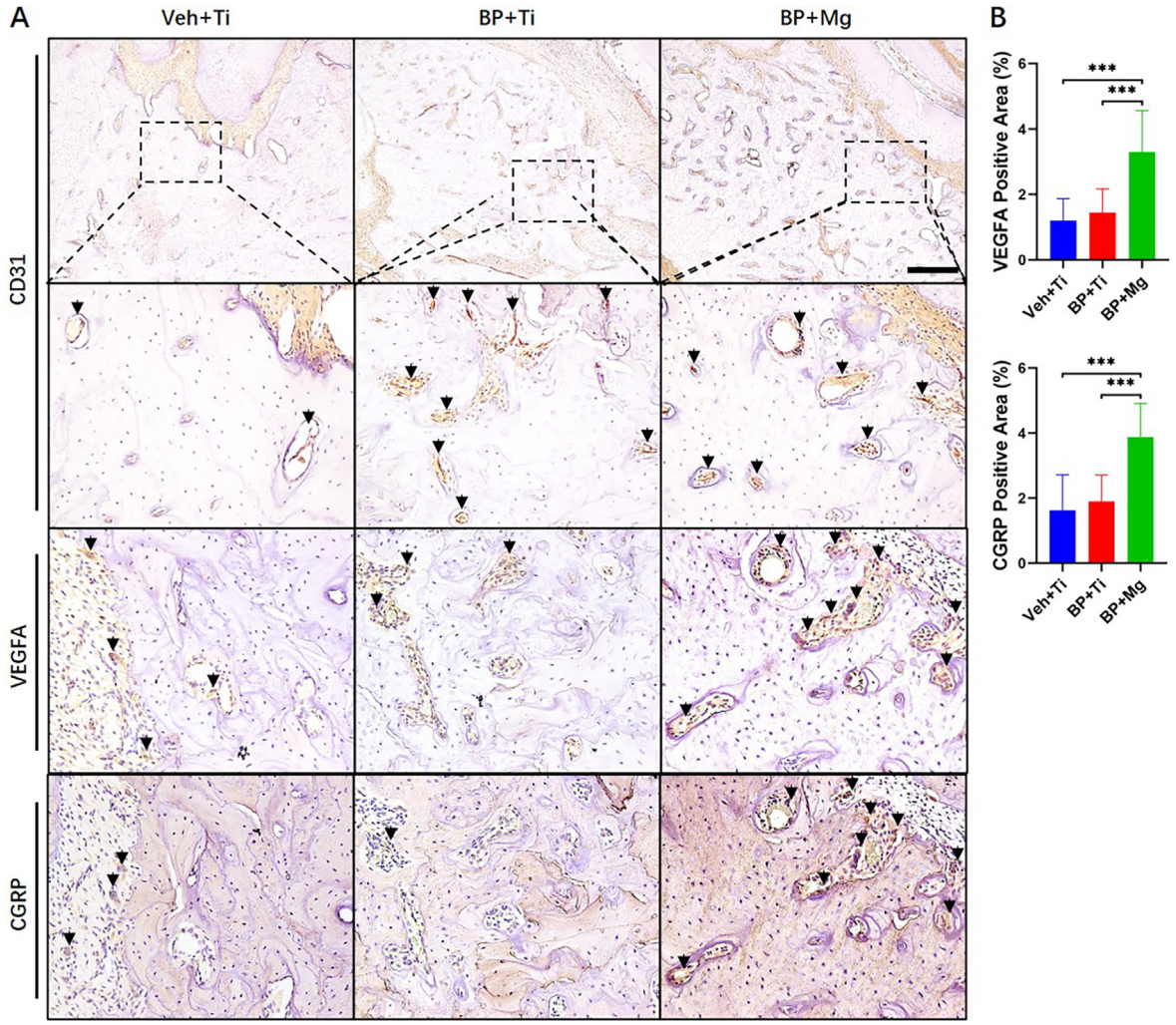

Fig. 3. VEGFA and CGRP expression compared among Veh + Ti, BP + Ti and BP + Mg groups (A) Representative images of IHC staining of CD31, VEGFA and CGRP in three groups, respectively. Black arrow points the positive stained cell. Scale bar: 400 μm (B) Corresponding quantitative data of VEGFA and CGRP. Column and bar indicate mean and SD, respectively. n = 5 for each group, by One-way ANOVA with Bonferroni *post hoc* test. ***, p < 0.001.

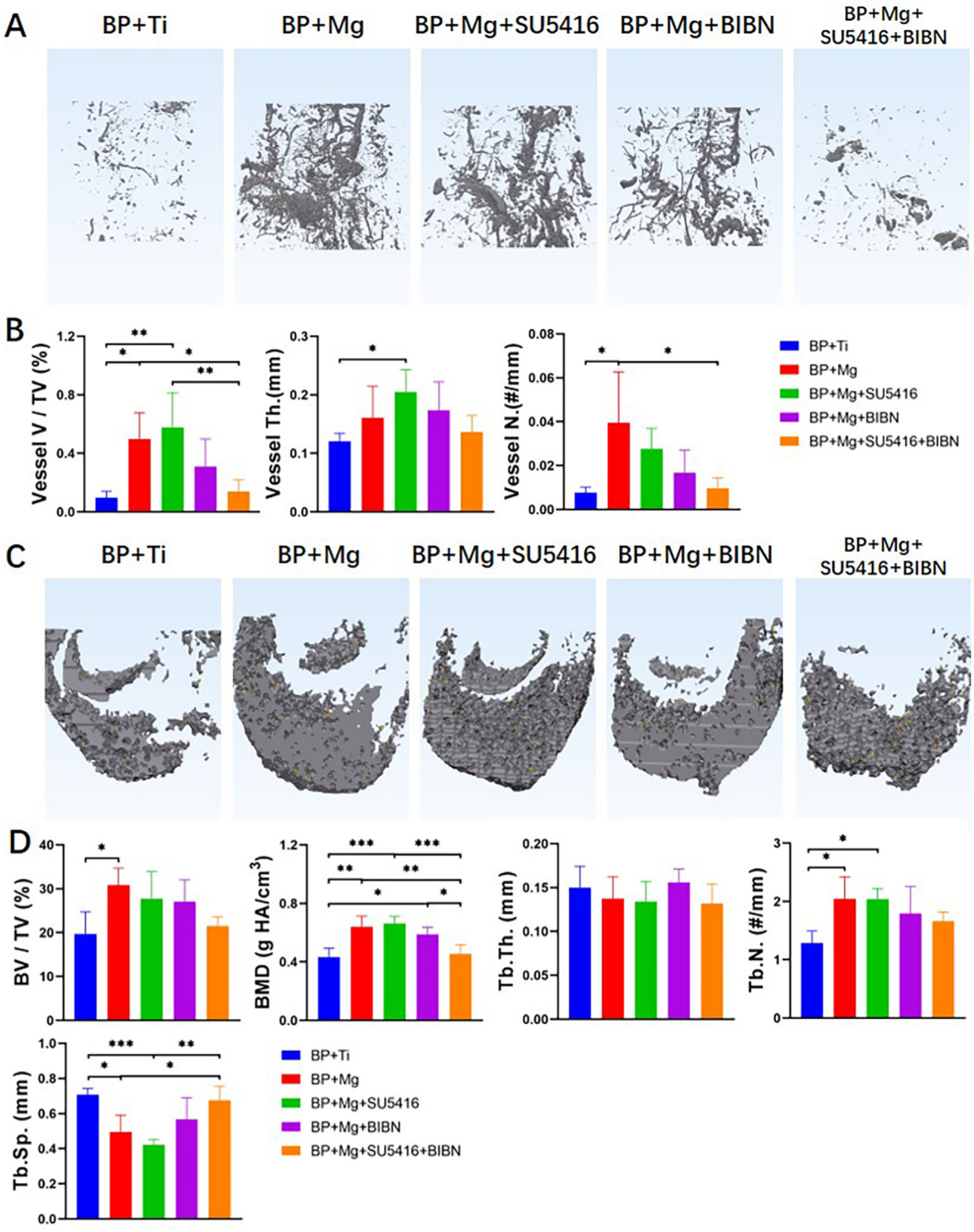

Fig. 4. Mg enhanced angiogenesis and coupled osteogenesis in MRONJ, which could be inhibited by blocking VEGF receptor-2 and CGRP receptor simultaneously, as indicated by micro-CT based angiography and bone histomorphometry analysis (A) Representative 3D reconstructed images of micro-CT based angiography showing the differences of vessel volume compared among the BP + Ti, BP + Mg, and BP + Mg + inhibitor/antagonist groups at 8 weeks after surgery. Scale bar: 5 mm (B) Quantitative analysis of angiography in different groups at 8 weeks after surgery (C) Representative 3D reconstructed images showing the differences of newly formed bone in the defect compared among groups at 8 weeks after surgery. Scale bar: 1 mm (D) Quantitative analysis of newly formed bone in different groups at 8 weeks after surgery. SU5416, VEGF receptor-2 inhibitor; BIBN, CGRP receptor antagonist. Column and bar indicate mean and SD, respectively. n = 4–5 for each group, by One-way ANOVA with Bonferroni *post hoc* test. *, $p < 0.05$; **, $p < 0.01$; ***, $p < 0.001$.

BP + Mg + BIBN group 8 weeks after surgery, as compared to the BP + Ti group and BP + Mg + SU5416+BIBN group (Fig. 4).

Quantitative micro-CT-based angiography results showed that percentages of vessel volume in the BP + Ti group and BP + Mg + SU5416+BIBN group were significantly lower than that of the BP + Mg group and BP + Mg + SU5416 group at 8 weeks after surgery. There was no significant difference in vessel volume percentage among the BP + Ti group, BP + Mg + BIBN group, and BP + Mg + SU5416+BIBN group (Fig. 4B). Meanwhile, the results of bone defect repair demonstrated significantly reduced BMD in the BP + Ti group and BP + Mg + SU5416+BIBN group at 8 weeks after surgery, indicated by micro-CT bone analysis (Fig. 4D).

3.4. VEGF- and CGRP-mediated angiogenesis can be responsible for Mg-alleviated MRONJ-like lesion development

At 8 weeks after surgery, incidences of MRONJ-like lesion in BP + Ti, BP + Mg, BP + Mg + SU5416, BP + Mg + BIBN, and BP + Mg + SU5416+BIBN groups were 100%, 25%, 40%, 20% and 100%, respectively. All rats in the BP + Ti group and BP + Mg + SU5416+BIBN group developed MRONJ-like lesions, while the BP + Mg group, BP + Mg + SU5416 group, and BP + Mg + BIBN group had significantly reduced occurrence of MRONJ-like lesions (Fig. 5A). Histology results showed a significantly increased ratio of empty lacunae and N. Empty Lacunae/B.Ar in the BP + Ti group and BP + Mg + SU5416+BIBN group, as compared to the BP + Mg group, BP + Mg + SU5416 group, and BP + Mg + BIBN group (Fig. 5B). Meanwhile, no significant difference in the expressions of VEGFA or CGRP among groups implanted with Mg rods (Fig. 5C and D; Negative controls without primary antibodies were shown in Appendix Fig. 1B). These results indicated that the Mg-induced alleviation of MRONJ-like lesion development was abrogated by simultaneously blocking VEGF receptor-2 and CGRP receptors. Furthermore, no remarkable difference in alveolar bone necrosis degree was observed among the BP + Mg and single inhibitor/antagonist applied groups, suggesting that the VEGF and CGRP played similar and complementary roles in the Mg-induced angiogenesis (Fig. 5E).

4. Discussion

In this study, we established a novel animal model to simulate a MRONJ-risk patient receiving jaw surgeries of dental extraction, implant fixation and bone defect creation, based on conventional MRONJ models in rodents [24,25]. The dosage of BP therapy received by rats was converted from human dosage, and 8 weeks as the diagnosis of MRONJ-like lesion was utilized simulating human diagnostic criteria of MRONJ and ensuring repeatability. We found that the BP-treated rats implanted with

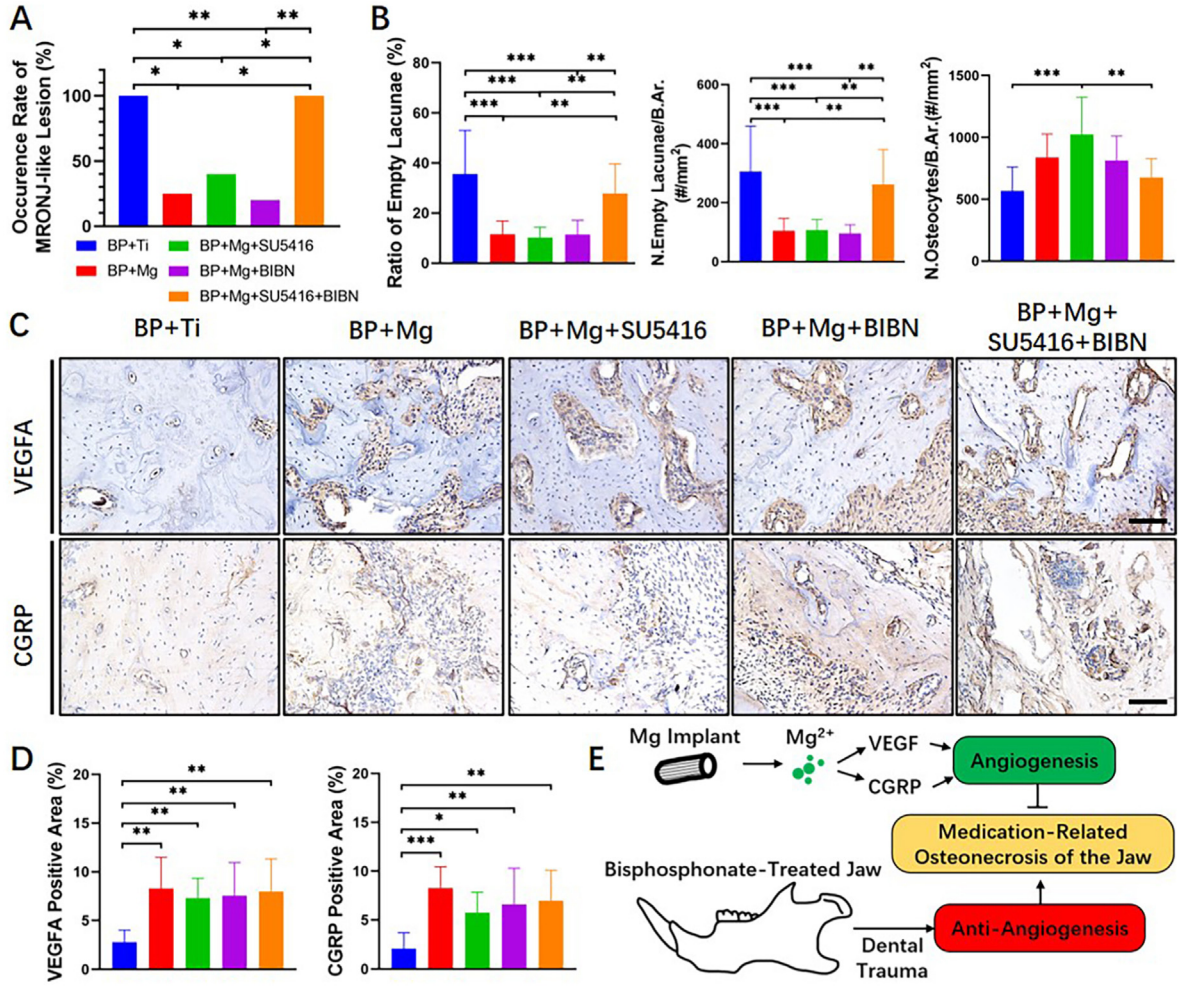

Fig. 5. Mg-alleviated MRONJ-like lesion development, possibly due to angiogenesis and osteogenesis (A) Occurrence rate of MRONJ-like lesion in the BP + Ti, BP + Mg, and BP + Mg + inhibitor/antagonist groups at 8 weeks after surgery (B) Histomorphometric assessments on the degree of alveolar bone necrosis among groups (H&E staining) (C) IHC staining of VEGFA (brown) and CGRP (brown) in the alveolar bone region in each group at 8 weeks after surgery. Scale bar: 100 μm (D) Corresponding quantitative data from (C). Column and bar indicate mean and SD, respectively. n = 4–5 for each group, by Chi-square test (A), and One-way ANOVA with Bonferroni *post hoc* test (B and D). **, $p < 0.01$; ***, $p < 0.001$ (E) Illustration of the underlying mechanism of biodegradable magnesium implant on attenuating the development of MRONJ via VEGF- and CGRP-mediated angiogenesis.

Mg rod had significantly reduced rate of MRONJ-like lesion occurrence and alleviated histological necrotic degree in the extraction site, through upregulating VEGF- and CGRP-mediated angiogenesis. To the best of our knowledge, this is the first study investigating the effects of Mg implants on MRONJ and the underlying mechanism.

To explore the pathogenesis of MRONJ in rodents, systematic reviews and meta-analyses summarize that the incidence of osteonecrosis associated with ZA monotherapy and ZA + DX combination therapy ranged from 30% to 100%, and mucosal defects with exposed bone, more necrotic bone with increased empty lacunae, decreased numbers of osteocytes, and severe infiltration of polymorphonuclears, are the most commonly observed pathological findings of MRONJ-like lesions [24,25]. In our study, all rats in BP + Ti group developed MRONJ-like lesions 8 weeks postoperatively, with similar histological features as observed in MRONJ patients. As expected, reduced occurrence rate of MRONJ-like lesion, empty lacunae ratio, and empty lacunae number per B.Ar was found in the BP-treated rats implanted with a Mg rod. Notably, our results also demonstrated a significantly decreased number of TRAP-positive osteoclasts in the Mg group. Some studies show that ZA therapy significantly increased the number of osteoclasts in the tooth extraction sockets 4 weeks after extraction than control [26,27], and the anti-osteoclastogenic effect of Mg [28,29] also could explain our results. Besides, numerous vessel-like tissues in the alveolar bone region were observed in the group implanted with Mg rods, companied with highly expressed VEGFA and CGRP. As important signal protein and sensory neuropeptides in angiogenesis, the Mg-induced VEGFA and CGRP might be involved in the attenuation of MRONJ-like lesions.

Mg possesses multiple osteopromotive properties in bone tissue regeneration [17,30]. The previous work done by our team showed that Mg ion improved the healing in bone fracture and ligament reconstruction by upregulating CGRP [18,31,32], and recently the CGRP-FAK-VEGF signaling axis linking sensory nerve and endothelial cells was further revealed to be responsible for the Mg-accelerated bone defect repair during distraction osteogenesis [20]. In our present *in vivo* experiments injected with inhibitor and/or antagonist, either injection of VEGF receptor-2 inhibitor or CGRP receptor antagonist could not block the Mg-induced angiogenesis and coupled osteogenesis in the BP-treated jawbone, and the Mg-enhanced tissue regeneration could only be blocked by the combined action of VEGF receptor-2 inhibitor and CGRP receptor antagonist, which were consistent with the occurrence rate and histological results of MRONJ-like lesion. It indicated that the main mechanism responsible for alleviating MRONJ-like lesion development was the enhancement of angiogenesis induced by Mg, which might be mediated by VEGF and CGRP, respectively. On one hand, either Mg-upregulated CGRP released from sensory nerve [20,33,34] or direct Mg ion stimulation on bone marrow stromal cells and endothelial cells [35–37] can upregulate VEGF, thus leading to angiogenesis. On the other hand, activation of the CGRP receptor also results in Gαs-mediated activation of adenylate cyclase in endothelial cells, inflammatory cells, and vascular smooth muscle cells, causing a subsequent increase in cyclic adenosine monophosphate and activation of nitric oxide synthase [38]. And nitric oxide promotes new vessel formation via cyclic guanosine monophosphate-protein kinase G pathway [39,40]. In this BP-treated model, the VEGF- and CGRP-mediated angiogenic effects might have equally important roles in attenuating the development of MRONJ, possibly via endothelial cells, which warrants further investigation.

Nevertheless, there were several limitations in this study. Firstly, the concentration of Mg ion derived from the implant in the mandible was unknown. Conflicting results of the osteogenic capacity of Mg ion have been observed by some studies, which indicate multiple roles of Mg ion with different concentrations in the complex biological process of bone healing [41–43]. Secondly, although most MRONJ studies are using rodent animals, there is still a debate concerning the use of small animal models for MRONJ research due to different anatomy and metabolism from humans. Since the unique features of the human jawbone can be responsible for the specific occurrence site of MRONJ [44], preclinical studies on rodents lacking the Haversian canal in the mandible need more pieces of evidence before clinical investigations [45].

In conclusion, our study demonstrated for the first time that the biodegradable Mg implant could alleviate the development of MRONJ-like lesions, possibly via upregulating VEGF- and CGRP-mediated angiogenesis. Mg-based implants have the potential to be developed as a novel internal fixation device for patients at the risk of MRONJ. Further studies focusing on the exact mechanisms underlying the effects of Mg on MRONJ are needed.

Declaration of competing interest

The author(s) have no conflicts of interest relevant to this article.

Acknowledgements

The project was supported by the University of Hong Kong Seed Fund for Basic Research (201811159067, 201910159037).

Appendix A. Supplementary data

Supplementary data to this article can be found online at https://doi.org/10.1016/j.jot.2022.03.004.

References

[1] Ruggiero SL, Dodson TB, Fantasia J, Goodday R, Aghaloo T, Mehrotra B, et al. American Association of Oral and Maxillofacial Surgeons position paper on medication-related osteonecrosis of the jaw–2014 update. J Oral Maxillofac Surg 2014;72(10):1938–56.
[2] Otto S, Pautke C, Van den Wyngaert T, Niepel D, Schiodt M. Medication-related osteonecrosis of the jaw: prevention, diagnosis and management in patients with cancer and bone metastases. Cancer Treat Rev 2018;69:177–87.
[3] Coleman R, Woodward E, Brown J, Cameron D, Bell R, Dodwell D, et al. Safety of zoledronic acid and incidence of osteonecrosis of the jaw (ONJ) during adjuvant therapy in a randomised phase III trial (AZURE: BIG 01-04) for women with stage II/III breast cancer. Breast Cancer Res Treat 2011;127(2):429–38 [eng].
[4] Mauri D, Valachis A, Polyzos IP, Polyzos NP, Kamposioras K, Pesce LL. Osteonecrosis of the jaw and use of bisphosphonates in adjuvant breast cancer treatment: a meta-analysis. Breast Cancer Res Treat 2009;116(3):433–9 [eng].
[5] Scagliotti GV, Hirsh V, Siena S, Henry DH, Woll PJ, Manegold C, et al. Overall survival improvement in patients with lung cancer and bone metastases treated with denosumab versus zoledronic acid: subgroup analysis from a randomized phase 3 study. J Thorac Oncol : Off Publ Int Assoc Stud Lung Cancer 2012;7(12):1823–9 [eng].
[6] Lopez-Olivo MA, Shah NA, Pratt G, Risser JM, Symanski E, Suarez-Almazor ME. Bisphosphonates in the treatment of patients with lung cancer and metastatic bone disease: a systematic review and meta-analysis. Support Care Cancer 2012;20(11):2985–98.
[7] Morgan GJ, Davies FE, Gregory WM, Cocks K, Bell SE, Szubert AJ, et al. First-line treatment with zoledronic acid as compared with clodronic acid in multiple myeloma (MRC Myeloma IX): a randomised controlled trial. Lancet 2010;376(9757):1989–99.
[8] Khan AA, Morrison A, Kendler DL, Rizzoli R, Hanley DA, Felsenberg D, et al. Case-based review of osteonecrosis of the jaw (ONJ) and application of the international recommendations for management from the international task force on ONJ. J Clin Densitom 2017;20(1):8–24.
[9] Wutzl A, Pohl S, Sulzbacher I, Seemann R, Lauer G, Ewers R, et al. Factors influencing surgical treatment of bisphosphonate-related osteonecrosis of the jaws. Head Neck 2012;34(2):194–200 [eng].
[10] Yamada S-I, Kurita H, Kondo E, Suzuki S, Nishimaki F, Yoshimura N, et al. Treatment outcomes and prognostic factors of medication-related osteonecrosis of the jaw: a case- and literature-based review. Clin Oral Invest 2019;23(8):3203–11 [eng].
[11] Graziani F, Vescovi P, Campisi G, Favia G, Gabriele M, Gaeta GM, et al. Resective surgical approach shows a high performance in the management of advanced cases of bisphosphonate-related osteonecrosis of the jaws: a retrospective survey of 347 cases. J Oral Maxillofac Surg 2012;70(11):2501–7.
[12] Yarom N, Shapiro CL, Peterson DE, Van Poznak CH, Bohlke K, Ruggiero SL, et al. Medication-related osteonecrosis of the jaw: MASCC/ISOO/ASCO clinical practice guideline. J Clin Oncol 2019;37(25):2270–90 [eng].
[13] Kang M-H, Lee D-K, Kim C-W, Song I-S, Jun S-H. Clinical characteristics and recurrence-related factors of medication-related osteonecrosis of the jaw. J Kor Assoc Oral Maxillofac Surg 2018;44(5):225–31 [eng].
[14] Mücke T, Koschinski J, Deppe H, Wagenpfeil S, Pautke C, Mitchell DA, et al. Outcome of treatment and parameters influencing recurrence in patients with bisphosphonate-related osteonecrosis of the jaws. J Cancer Res Clin Oncol 2011;137(5):907–13 [eng].

[15] Zhao D, Huang S, Lu F, Wang B, Yang L, Qin L, et al. Vascularized bone grafting fixed by biodegradable magnesium screw for treating osteonecrosis of the femoral head. Biomaterials 2016;81:84–92.
[16] Huang S, Wang B, Zhang X, Lu F, Wang Z, Tian S, et al. High-purity weight-bearing magnesium screw: translational application in the healing of femoral neck fracture. Biomaterials 2020;238:119829.
[17] Wang JL, Xu JK, Hopkins C, Chow DH, Qin L. Biodegradable magnesium-based implants in orthopedics-A general review and perspectives. Adv Sci 2020;7(8): 1902443.
[18] Zhang Y, Xu J, Ruan YC, Yu MK, O'Laughlin M, Wise H, et al. Implant-derived magnesium induces local neuronal production of CGRP to improve bone-fracture healing in rats. Nat Med 2016;22(10):1160–9.
[19] Tuo Y, Guo X, Zhang X, Wang Z, Zhou J, Xia L, et al. The biological effects and mechanisms of calcitonin gene-related peptide on human endothelial cell. J Recept Signal Transduct Res 2013;33(2):114–23.
[20] Ye L, Xu J, Mi J, He X, Pan Q, Zheng L, et al. Biodegradable magnesium combined with distraction osteogenesis synergistically stimulates bone tissue regeneration via CGRP-FAK-VEGF signaling axis. Biomaterials 2021;275:120984.
[21] Khan AA, Morrison A, Hanley DA, Felsenberg D, McCauley LK, O'Ryan F, et al. Diagnosis and management of osteonecrosis of the jaw: a systematic review and international consensus. J Bone Miner Res 2015;30(1):3–23.
[22] Jabbour Z, El-Hakim M, Henderson JE, de Albuquerque Jr RF. Bisphosphonates inhibit bone remodeling in the jaw bones of rats and delay healing following tooth extractions. Oral Oncol 2014;50(5):485–90.
[23] Kim JW, Tatad JCI, Landayan MEA, Kim SJ, Kim MR. Animal model for medication-related osteonecrosis of the jaw with precedent metabolic bone disease. Bone 2015; 81:442–8.
[24] Kuroshima S, Sasaki M, Murata H, Sawase T. Medication-related osteonecrosis of the jaw-like lesions in rodents: a comprehensive systematic review and meta-analysis. Gerodontology 2019;36(4):313–24.
[25] Poubel V, Silva CAB, Mezzomo LAM, De Luca Canto G, Rivero ERC. The risk of osteonecrosis on alveolar healing after tooth extraction and systemic administration of antiresorptive drugs in rodents: a systematic review. J Cranio-Maxillo-Fac Surg 2018;46(2):245–56.
[26] Soundia A, Hadaya D, Esfandi N, de Molon RS, Bezouglaia O, Dry SM, et al. Osteonecrosis of the jaws (ONJ) in mice after extraction of teeth with periradicular disease. Bone 2016;90:133–41.
[27] Park S, Kanayama K, Kaur K, Tseng H-CH, Banankhah S, Quje DT, et al. Osteonecrosis of the jaw developed in mice. J Biol Chem 2015;290(28):17349–66.
[28] Zhai Z, Qu X, Li H, Yang K, Wan P, Tan L, et al. The effect of metallic magnesium degradation products on osteoclast-induced osteolysis and attenuation of NF-kappaB and NFATc1 signaling. Biomaterials 2014;35(24):6299–310.
[29] Wu L, Feyerabend F, Schilling AF, Willumeit-Römer R, Luthringer BJC. Effects of extracellular magnesium extract on the proliferation and differentiation of human osteoblasts and osteoclasts in coculture. Acta Biomater 2015;27:294–304 [eng].
[30] Zhao D, Witte F, Lu F, Wang J, Li J, Qin L. Current status on clinical applications of magnesium-based orthopaedic implants: a review from clinical translational perspective. Biomaterials 2017;112:287–302.
[31] Tian L, Sheng Y, Huang L, Chow DH, Chau WH, Tang N, et al. An innovative Mg/Ti hybrid fixation system developed for fracture fixation and healing enhancement at load-bearing skeletal site. Biomaterials 2018;180:173–83.
[32] Wang J, Xu J, Wang X, Sheng L, Zheng L, Song B, et al. Magnesium-pretreated periosteum for promoting bone-tendon healing after anterior cruciate ligament reconstruction. Biomaterials 2020;268:120576 [eng].
[33] Rhee SH, Ma EL, Lee Y, Tache Y, Pothoulakis C, Im E. Corticotropin releasing hormone and urocortin 3 stimulate vascular endothelial growth factor expression through the cAMP/CREB pathway. J Biol Chem 2015;290(43):26194–203.
[34] Amano H, Ando K, Minamida S, Hayashi I, Ogino M, Yamashina S, et al. Adenylate cyclase/protein kinase A signaling pathway enhances angiogenesis through induction of vascular endothelial growth factor in vivo. Jpn J Pharmacol 2001; 87(3):181–8.
[35] Xu L, Willumeit-Römer R, Luthringer-Feyerabend BJC. Effect of magnesium-degradation products and hypoxia on the angiogenesis of human umbilical vein endothelial cells. Acta Biomater 2019;98:269–83.
[36] Yoshizawa S, Brown A, Barchowsky A, Sfeir C. Magnesium ion stimulation of bone marrow stromal cells enhances osteogenic activity, simulating the effect of magnesium alloy degradation. Acta Biomater 2014;10(6):2834–42.
[37] Zheng LZ, Wang JL, Xu JK, Zhang XT, Liu BY, Huang L, et al. Magnesium and vitamin C supplementation attenuates steroid-associated osteonecrosis in a rat model. Biomaterials 2020;238:119828.
[38] Majima M, Ito Y, Hosono K, Amano H. CGRP/CGRP receptor antibodies: potential adverse effects due to blockade of neovascularization? Trends Pharmacol Sci 2019; 40(1):11–21.
[39] Ziche M, Morbidelli L. Nitric oxide and angiogenesis. J Neuro Oncol 2000;50(1–2): 139–48 [eng].
[40] Ghimire K, Altmann HM, Straub AC, Isenberg JS. Nitric oxide: what's new to NO? Am J Physiol Cell Physiol 2017;312(3):C254–62.
[41] Leidi M, Dellera F, Mariotti M, Maier JAM. High magnesium inhibits human osteoblast differentiation in vitro. Magnes Res 2011;24(1):1–6 [eng].
[42] Li RW, Kirkland NT, Truong J, Wang J, Smith PN, Birbilis N, et al. The influence of biodegradable magnesium alloys on the osteogenic differentiation of human mesenchymal stem cells. J Biomed Mater Res 2014;102(12):4346–57 [eng].
[43] Zhang J, Tang L, Qi H, Zhao Q, Liu Y, Zhang Y. Dual function of magnesium in bone biomineralization. Adv Healthc Mater 2019;8(21):e1901030 [eng].
[44] Japanese Allied Committee on Osteonecrosis of the J, Yoneda T, Hagino H, Sugimoto T, Ohta H, Takahashi S, et al. Antiresorptive agent-related osteonecrosis of the jaw: position paper 2017 of the Japanese allied committee on osteonecrosis of the jaw. J Bone Miner Metabol 2017;35(1):6–19.
[45] Bagi CM, Berryman E, Moalli MR. Comparative bone anatomy of commonly used laboratory animals: implications for drug discovery. Comp Med 2011;61(1):76–85 [eng].